Electronic Supplementary Material (ESI) for Lab on a Chip.

Supplementary Information

Contactless, programmable acoustofluidic manipulation of objects on water

Peiran Zhang,[a] Chuyi Chen[a], Feng Guo,[b] Julien Philippe[c], Yuyang Gu,[a] Zhenhua Tian,[a] Hunter Bachman,[a] Liqiang Ren[b], Shujie Yang,[a] Zhanwei Zhong,[d] Po-Hsun Huang,[a] Nicholas Katsanis,[c] Krishnendu Chakrabarty,[d] and Tony Jun Huang[a§]

[a.] Department of Mechanical Engineering and Material Science, Duke University, NC 27707, USA.
[b.] Department of Engineering Sciences and Mechanics, The Pennsylvania State University, PA, 16801, USA.
[c.] Center for Human Disease Modelling, Duke University Medical Center, Durham, NC, 27701, USA.
[d.] Department of Electrical and Computer Engineering, Duke University, NC, 27708, USA

Part 1. Supplementary Note S1

Numerical Simulation.

To understand the flow patterns induced by the hollow-square-shaped interdigital transducers in the water, a numerical simulation of acoustic streaming was conducted. The computational domain is shown in Fig. S1. Only a quarter of the interdigital transducer electrodes was studied in the simulation because the geometry of the IDTs is symmetric about both the *x* and *y* axes. The substrate vibration activated by the hollow-square-shaped IDTs was governed by the constructive equations of piezoelectric material in the stress-charge form. The acoustic field and acoustic streaming pattern were governed by the first- and second-order equations, respectively, as deduced from perturbation theory[1] based on the fluid mass and momentum continuity equations[2]. The "slip velocity method"[3] based on the boundary-driven streaming theory[4,5] was applied to reduce the calculation amount for the simulation. COMSOL Multiphysics 5.2a was employed for the simulation. First, the coupled substrate vibration in Ω_1 and acoustic field in the inner streaming domain (Ω_2) was solved in the frequency domain. Then, the stationary inner streaming was solved based on the acoustic field in Ω_1. At last, applying the inner streaming pattern on Σ_2 as the actuation, the outer streaming in the Ω_3 was solved. The details of the theoretical model and simulation strategy are stated elsewhere[3]. The numerical solution of the outer streaming pattern induced by the whole IDT on the top of the water domain (water-air interface) is shown in Fig. 3f. The numerical result shows that the water loading on the IDTs flows away from the side of the IDT perpendicularly to the IDT electrodes. As such, the objects (oil droplets) loading on the water will be pushed along the direction of the streaming pattern.

Part 2. Supplementary figures

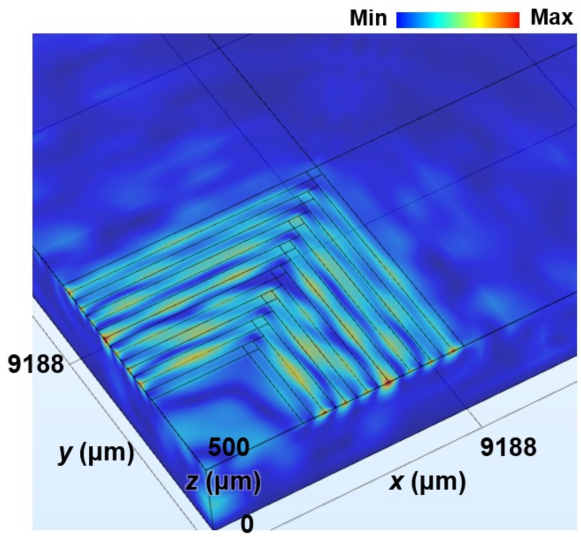

Figure S1. Simulation showing a quarter view of the displacement distribution of an excited transducer.

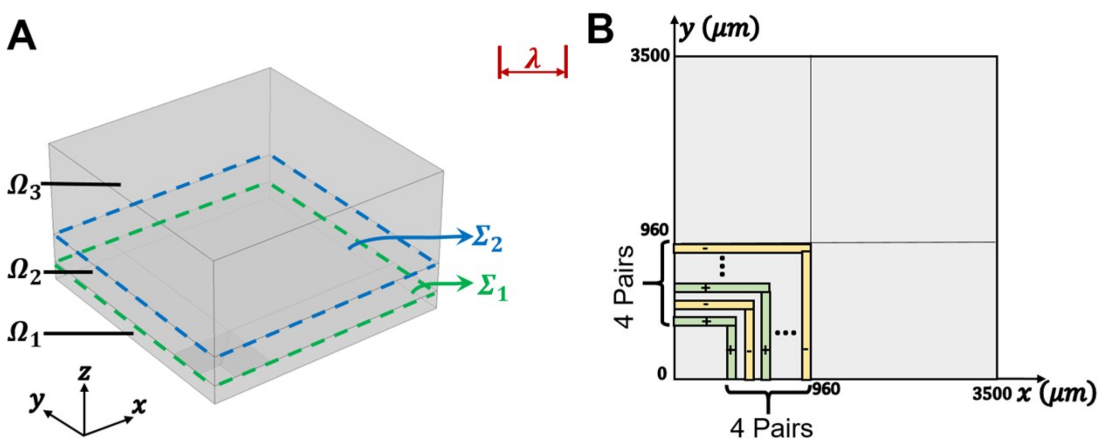

Figure S2. Schematic of (A) the computational domain and (B) electrode setup on the top of the substrate (Σ_1). (A) $LiNbO_3$ substrate and fluid domain containing a quarter of the interdigital transducers. The Ω_1 is the 0.5-mm thick $LiNbO_3$ substrate, the Ω_2 indicates inner streaming domain of thickness four times that of the boundary streaming layer, and Ω_3 is the outer streaming domain. Σ_1 indicates the top of the substrate and Σ_2 indicates the top of the inner streaming domain (Ω_2). (B) The geometry of four pairs IDTs setup on Σ_1. The finger width is 37.5 μm which corresponds to the 24.2 MHz frequency.

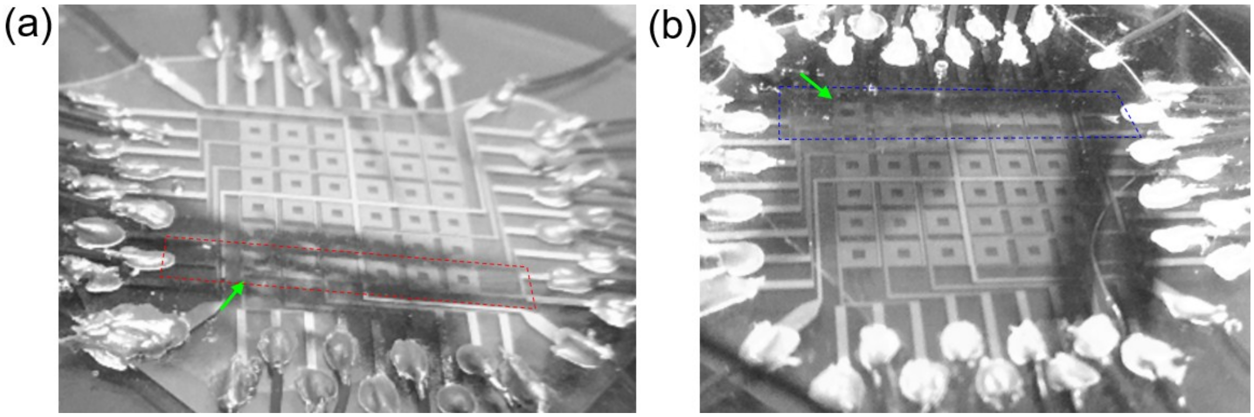

Figure S3. Photos showing the crossing ripples over an excited transducer unit. The green arrow indicates the position of the excited transducer. The ripples on the surface of water are visualized by the reflection of illumination on the gold electrodes whiling manually shedding a shadow over the region of interest on the camera. Photo (a) and (b) were taken from two different angles. The red and blue dashed boxes indicates the position of the ripples.

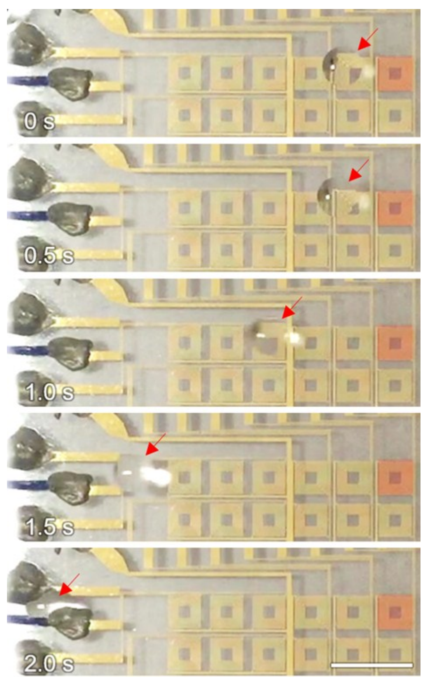

Figure S4. The translation of a mineral oil droplet on across the transducer array. Scale bar: 5 mm.

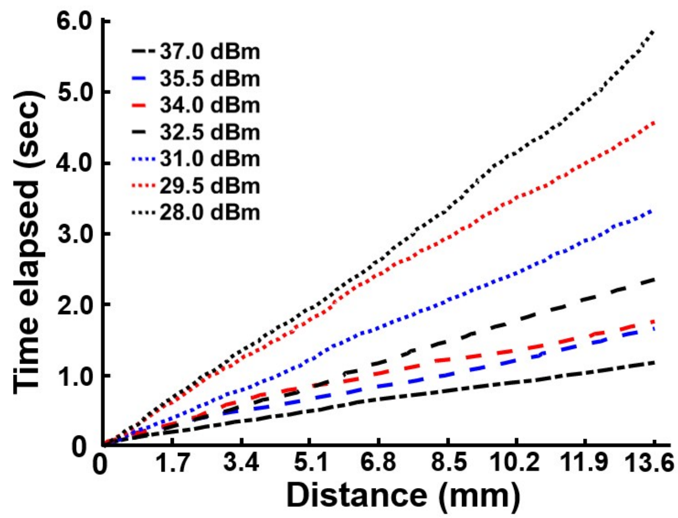

Figure S5. A diagram showing the relationships between distance and time for different excitation powers on a single transducer.

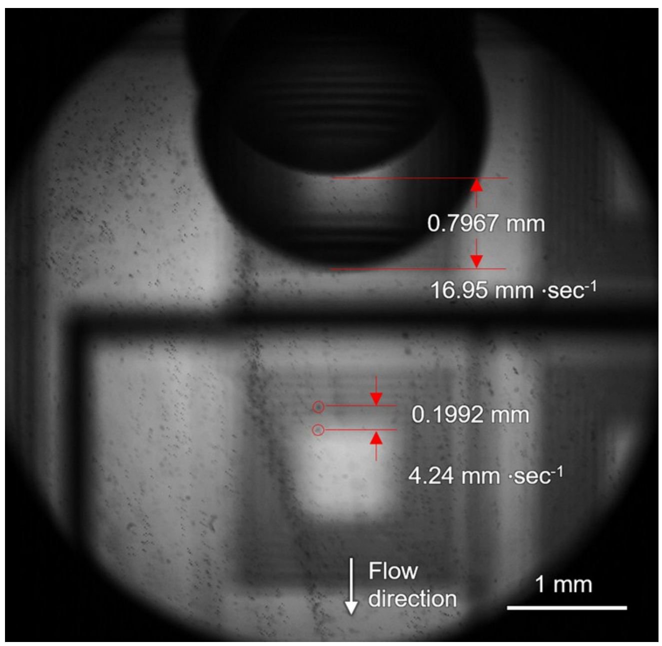

Figure S6. Particle tracking with a 1-µL mineral-oil droplet floating on the surface of water. The observed area is located at the 2nd and 3rd unit transducer from the excited IDT in the path of droplet translation.

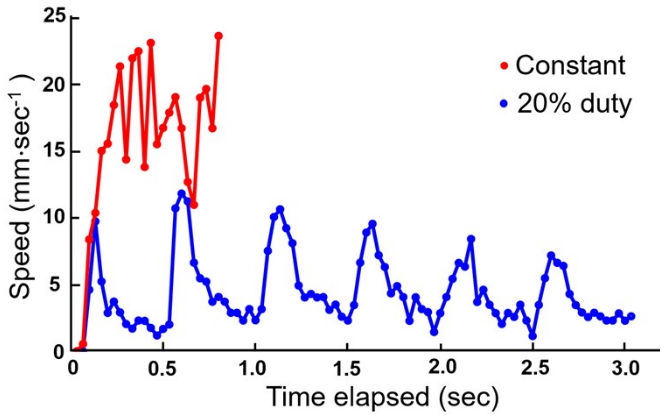

Figure S7. A diagram showing the relationships between the elapsed time and the traveling speed of a droplet upon the activation of the IDT using constant (red) and pulsed (blue) input signals (i.e., 2 Hz, 20 % duty ratio). Using the constant excitation signal, the droplet accelerated drastically within the first 0.3 seconds and reached a stable speed. Using the pulsed excitation signal, the speed of droplet oscillates periodically but with decreasing amplitude as travelling away from the transducer.

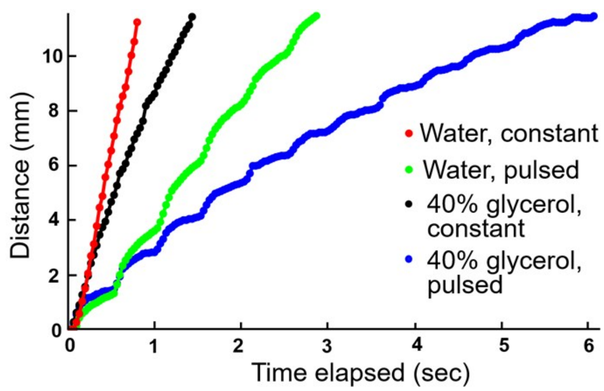

Figure S8. A diagram showing the relationships between the elapsed time and the traveling distance of a droplet floating on water and 40 % glycerol-water solution upon the activation of the IDT using constant and pulsed input signals (i.e., 2 Hz, 20 % duty ratio). With 40% glycerol, the viscosity of the carrier fluid increases to 3.72 cSt (20˚C), which is 3.7-fold higher than the viscosity of water (1 cSt, 20˚C). The droplet accelerates slower in the glycerol solution and can be used for the manipulation of droplets with higher positional resolution.

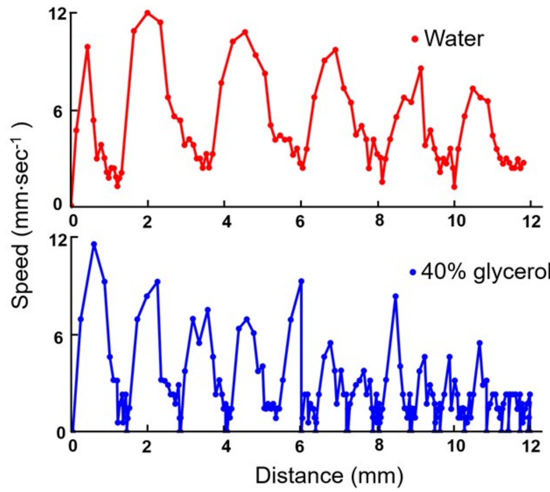

Figure S9. A diagram showing the relationships between the traveling distance and speed of a droplet floating on water (red) and 40 % glycerol-water solution (blue) upon the activation of the IDT using pulsed input signals (i.e., 2 Hz, 20% duty ratio).

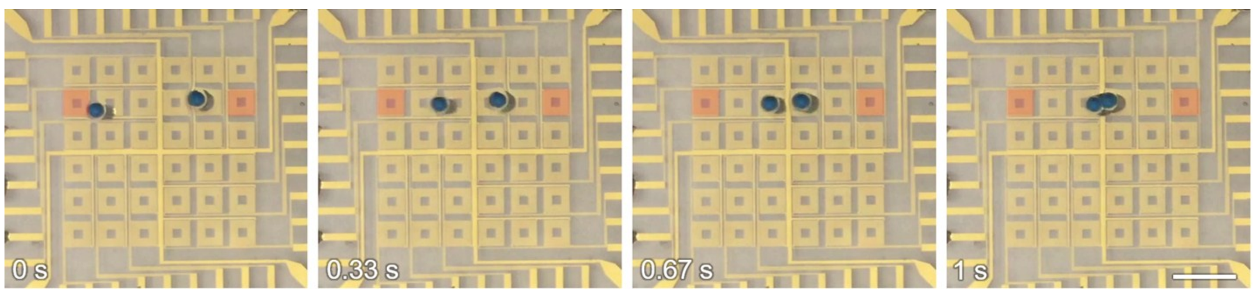

Figure S10. The time-lapsed merging process of two particle-containing droplets. The excited transducers are indicated by the red squares. Scale bar: 5 mm.

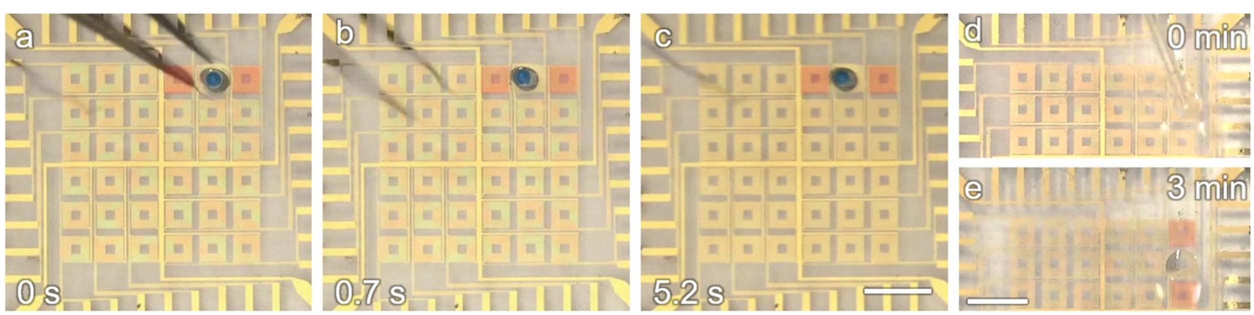

Figure S11. (a) – (b) The trapping of a particle-containing droplet using two transducers (red squares). (d) (e) A droplet being trapped for 3 minutes. Scale bars: 5 mm.

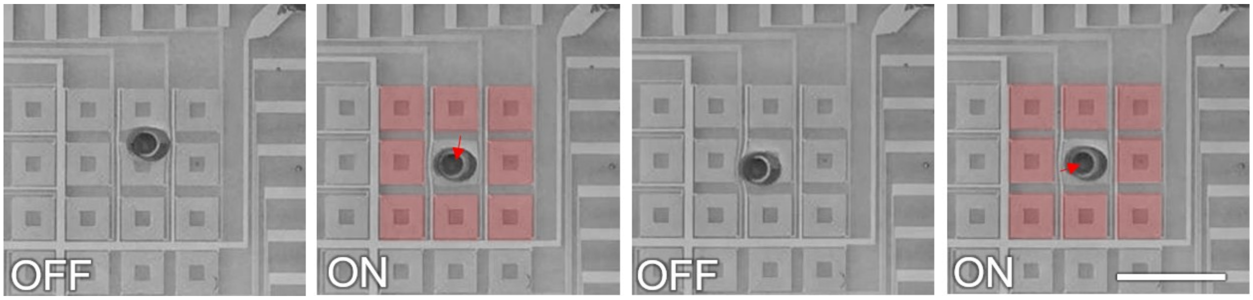

Figure S12. The repeated trap-release process of a particle-containing droplet using surrounding transducers. Scale bar: 5 mm.

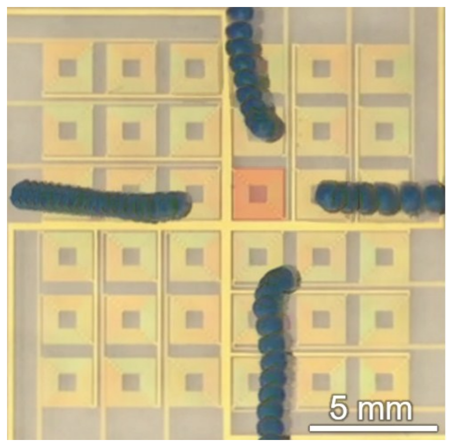

Figure S13. Stacked image showing the four-way actuation of four particle-containing oil droplets simultaneously using a unit-transducer (indicated by the red square). Unit-to-unit interference needs to be avoided for the simultaneous manipulation of multiple objects (i.e., more than one), potentially by spatiotemporal planning for droplet routing.

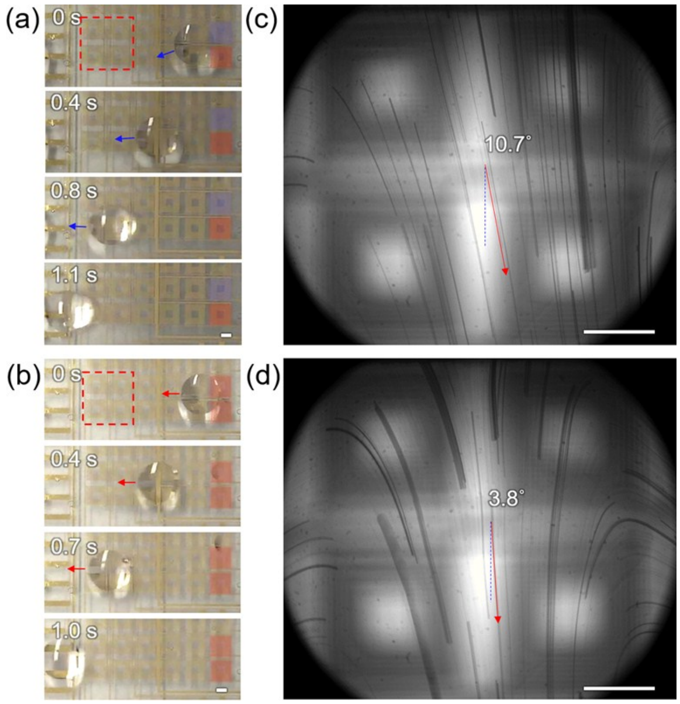

Figure S14. The time-lapsed translation process of a 4-μL mineral-oil droplet using two adjacent transducer with unbalanced (a) and balanced (b) amplitude of excitation signals. The corresponding flow-patterns on water-surface (red dashed boxes) are visualized by the stacked particle trajectories in (c) and (d). The unbalanced scenario has higher tilted angle (10.7˚) than the balanced scenario (3.8˚). Two images with a time interval of 47 ms are stacked together to calculate the speed of the surface flow and the droplet. The flow direction is indicated by the white arrow.

Part 3. Supplementary Movies

Movie S1. Translation of a 1-μL mineral-oil droplet across the transducer array by exciting one transducer using pulsed signal (i.e., 2 Hz, 20 % duty ratio).

Movie S2. Translation of a 1-μL mineral-oil droplet across the transducer array by exciting one transducer using pulsed signal with duty ratio from 10 % - 100 % (i.e., 2 Hz).

Movie S3. Merging of two particle-containing oil-droplets.

Movie S4. Drifting of a 1-μL mineral-oil droplet on 40% glycerol solution after being translated for two steps.

Movie S5. Trapping of a particle-containing oil droplet using two opposing unit-transducers.

Movie S6. Repeated trapping and releasing of a particle-containing oil droplet using eight surrounding unit-transducers.

Movie S7. Programmable translation of oil droplets writing “U”, “P”, “S”, and small “s” sequentially.

Movie S8. Multiport transportation of oil droplets.

Movie S9. Simultaneous rotation of two mineral-oil droplets.

References:

[1] W. L. Nyborg, in Nonlinear Acoustics, ed. M. F. Hamilton and D. T. Blackstock, Academic Press, San Diego, CA, 1998, 207–231.

[2] N. Nama, R. Barnkob, Z. Mao, C. J. Kähler, F. Costanzo and T. J. Huang, *Lab Chip*, 2015, **15**, 2700–2709.

[3] C. Chen, S.P. Zhang, Z. Mao, N. Nama, Y. Gu, P.H. Huang, Y. Jing, X. Guo, F. Costanzo, and T.J. Huang, *Lab Chip*, 2018, **18**, 3645-3654.

[4] S. S. Sadhal, *Lab Chip*, 2012, **12**, 2292–2300.

[5] O. Manor, L. Y. Yeo and J. R. Friend, *J. Fluid Mech.*, 2012, **707**, 482–495.